

# Observed and Theoretical Deformation Density Studies of the Aziridinyl, Benzene, and Phosphazene Rings in the Crystal Structure of the Benzene Solvate of Hexaaziridinylcyclotriphosphazene

T. Stanley Cameron,\* Bozena Borecka,† and Witold Kwiatkowski‡

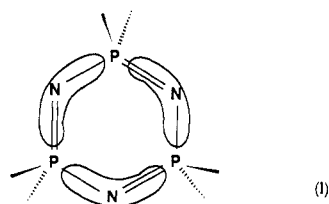
Contribution from the Department of Chemistry, Dalhousie University, Halifax, Nova Scotia, Canada B3H 4J3

Received August 27, 1993\*

**Abstract:** The crystal structure and the electron density of the benzene solvate of hexaaziridinylcyclotriphosphazene have been analyzed using single-crystal X-ray diffraction at 200 K with Mo K $\alpha$  radiation and an area detector to a resolution of  $\sin(\Theta_{\max})/\lambda = 1.25 \text{ \AA}^{-1}$ ; 17 639 measured reflections gave 4596 unique reflections with  $R_m = 0.027$ . A multipole atomic density model was fitted to 4038 reflections with  $I > 3\sigma(I)$  to give an  $R(F^2) = 0.039$ . The dynamic deformation densities of the trapped benzene molecule, the two unique three-membered aziridinyl rings, and the phosphazene ring have all been examined and are reported here for the first time. Those of the benzene and the aziridinyl groups conform to the expected density for these systems. These observations are used to validate the observations of the dynamic deformation density in the phosphazene ring. The observed dynamic deformation density in this ring corresponds to the density for the  $\pi/\pi'$  models with conjugation from a phosphorus atom, through a ring nitrogen atom to a second phosphorus, but with nodes at each of the phosphorus atoms. Theoretical dynamic deformation densities, derived from *ab initio* calculations and carried out on the simple aziridinyl and phosphazene rings, closely resemble the observed deformation densities.

## Introduction

Ever since Dewar, Lucken, and Whitehead proposed<sup>1</sup> their "island delocalization" model for the bonding in phosphazene rings, the exact nature of this bonding has been a subject for much discussion.<sup>2</sup> Dewar *et al.* showed that, in the cyclotriphosphazene, the  $\pi$  overlap between the d orbitals on the phosphorus atoms and the p orbitals on the nitrogen atoms in the ring would produce a  $\pi$  system above and below the plane of the ring which had nodes at each of the phosphorus atoms (I). Craig and Paddock



later added<sup>3</sup> the  $\pi'$  in-plane overlap which maintained the nodes at the phosphorus atom but suggested an extension of the  $\pi$  system within, and in the plane of, the ring. More detailed theoretical calculations since<sup>4,5</sup> support this combined  $\pi/\pi'$  model and suggest that the conjugation between the three-center islands is minor. There have been a number of studies of the influence on the bonding of substituents in the ring,<sup>6</sup> but it seems that the combined  $\pi/\pi'$  model is still the accepted explanation.<sup>7</sup> In the light of these theoretical models, we propose here to examine the bonding

\* Present address: Department of Chemistry, University of British Columbia, 2036 Main Mall, Vancouver BC, Canada V6T 1Y6.

† Present address: Medical Foundation of Buffalo, Inc., 73 High Street, Buffalo, NY 14203-1196.

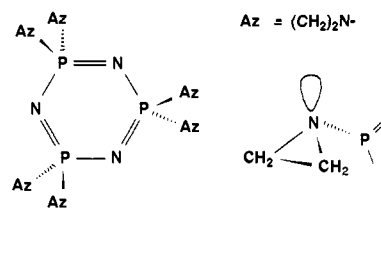
‡ Abstract published in *Advance ACS Abstracts*, January 15, 1994.

(1) Dewar, M. J. S.; Lucken, E. A. C.; Whitehead, M. A. *J. Chem. Soc.* **1960**, 2423.  
(2) Allcock, H. R. *Chem. Rev.* **1972**, 72, 315 and references therein.  
(3) Craig, D. P.; Paddock, N. L. *J. Chem. Soc.* **1962**, 4118.

(4) Faucher, J.-P.; Labarre, J.-F.; Shaw, R. A. *Z. Naturforsch.* **1976**, 31b, 677.  
(5) Allen, C. W. In *The Chemistry of Inorganic Homo- and Heterocycles*; Academic Press: London, 1987; Vol. 2, p 501 and references therein.

in a phosphazene ring through a low-temperature X-ray crystallographic study of the dynamic deformation density in the ring and to compare it with the theoretically calculated deformation density.

Hexaaziridinylcyclotriphosphazene (II) crystallizes in at least four different forms<sup>8</sup> which depend upon the solvent used. When it is recrystallized from benzene, it forms clear gemlike octahedral crystals which, at temperatures below 18 °C, are in space group<sup>9</sup>  $R\bar{3}$ . In the rhombohedral setting of this space group, the unit cell



contains just two phosphazenes and a single benzene molecule, with the center of each molecule on the 3-fold axis and with the two phosphazene molecules related by the inversion center on the axis. In addition, the center of the benzene ring coincides with this inversion center. The unit cell thus contains only one unique benzene carbon atom, one unique nitrogen and phosphorus atom in the phosphazene ring, and two unique aziridinyl groups. As a consequence of this arrangement, the benzene ring is sandwiched between the two phosphazene molecules which appear to hold it in place quite firmly<sup>10</sup> (Figure 1a). However, this benzene ring has six close neighbors from adjacent cells (Figure 1b), and these also severely restrict the prospect of librational motion for the

(6) See, for example: Dake, L. S.; Baer, D. R.; Ferris, K. F.; Friedrich, D. M. *J. Electron Spectrosc. Relat. Phenom.* **1990**, 51, 439.

(7) Corbridge, D. E. C. *PHOSPHORUS an outline of its chemistry*, 4th ed.; Elsevier: Amsterdam, 1990; p 437.

(8) Cameron, T. S.; Labarre, J.-F.; Graffeuil, M. *Acta Crystallogr.* **1982**, B38, 2000.

(9) Cameron, T. S.; Labarre, J.-F.; Graffeuil, M. *Acta Crystallogr.* **1982**, B38, 168.

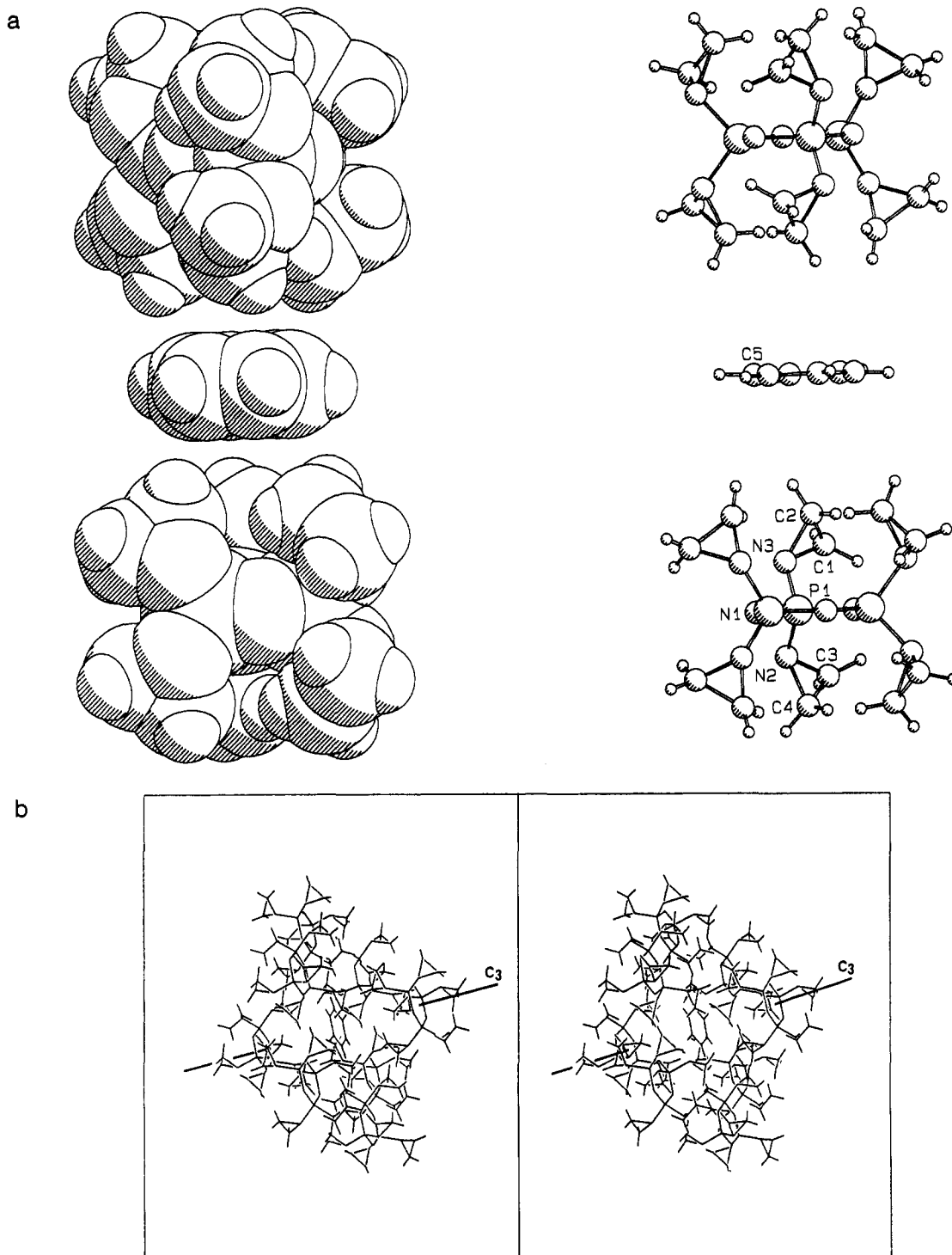


Figure 1. (a) Benzene securely trapped between two phosphazene molecules. (b) Local environment of the benzene ring.

benzene ring. This system is thus exceptionally well suited for an investigation of the bonding electron density. While the deformation density of benzene has not previously been derived from crystallographic measurements,<sup>11</sup> the expected density is well known, and the observation of this should act as an internal standard for the observations on the phosphazene. Similarly, while the deformation density on the three-membered aziridiny ring has also never been observed, excellent deformation density

(10) In the structure of this compound, determined at room temperature,<sup>9</sup> the anisotropic thermal parameters  $U_{ij}$  of the single unique carbon atom of the benzene molecule are 0.057(5), 0.050(5), and 0.056(6) which give essentially a spherical electron density at this site.

(11) The structure of benzene has been reported several times, most recently by: Jeffrey, G. A.; Ruble, J. R.; McMullan, R. K.; Pople, J. A. *Proc. R. Soc. London, A* 1987, 414, 47. See, also: Spackman, M. A. *Chem. Rev.* 1992, 92, 1769 (ref 144).

measurements have been made<sup>12</sup> on cyclopropane derivatives. Thus, by comparison, the determined deformation density on *both* of the two unique aziridiny groups can also be used to validate the phosphazene observations. The observed deformation densities can also now be compared with the densities calculated from theoretical studies.

#### Experimental Section

(i) **X-ray Data.** Although the crystal is rhombohedral, the X-ray data were collected as for a triclinic system. The data were collected from three different crystals, each under different conditions. The first two sets were collected on a CAD4 four-circle diffractometer, over a  $\theta$  range

(12) Seiler, P.; Belzner, J.; Bunz, U.; Szeimies, G. *Helv. Chim. Acta* 1988, 71, 2100.

Table 1. Crystal Data

formula	2P <sub>3</sub> N <sub>3</sub> (NC <sub>2</sub> H <sub>4</sub> ) <sub>6</sub> C <sub>6</sub> H <sub>6</sub>
molecular weight	852.72
crystal class	trigonal
space group	R $\bar{3}$ (hexagonal) (No. 148)
temperature (K)	200(1)
<i>a</i> (Å)	13.026(1)
<i>c</i> (Å)	20.759(1)
<i>V</i> (Å <sup>3</sup> )	3050.5(2)
<i>Z</i>	3
<i>d<sub>c</sub></i> (g cm <sup>-3</sup> )	1.393
<i>F</i> (000)	1350
<i>μ</i> (cm <sup>-1</sup> )	3.14
crystal size (mm)	0.02 × 0.02 × 0.02
diffractometer	RAXIS II-c
<i>λ</i> (Å) (Mo K $\alpha$ )	0.71069
$\theta$ range (deg)	0–63
sine $\theta/\lambda$ (Å <sup>-1</sup> )	1.25
take off angle (deg)	2.8
detector aperture (mm)	200 × 200
crystal to detector dist (mm)	59
detector off-axis angle (deg)	-28.5
scan	6° oscillations
no. of measrd refls	17639
no. of unique refls	4596
no. of unique refls $I > 3\sigma(I)$ <i>N<sub>ob</sub></i>	4038
<i>N'<sub>ob</sub></i> (3° < $\theta$ < 23°)	1000
<i>R<sub>merge</sub></i> (4596, 4038 refls)	0.027, 0.025
no. of variables, <i>N<sub>v</sub></i>	119
<i>N<sub>ob</sub>/N<sub>v</sub>, N'<sub>ob</sub>/N<sub>v</sub></i>	33.9, 8.4
weighting scheme	1/ $\sigma^2(F_o)$
Full Data (4038 refls), Regular Refinement	
highest peak diff Fourier (e Å <sup>-3</sup> )	0.47
agreement factors	
$R = (\sum   F_o  -  F_c  ) / (\sum  F_o )$	0.0430
$R_w = [\sum w( F_o  -  F_c )^2]^{1/2} / (\sum w F_o )^{1/2}$	0.0490
GOF = $[\sum ( F_o  -  F_c )^2 / (N_{ob} - N_v)]^{1/2}$	1.910
Full Data (1000 refls), Regular Refinement	
highest peak diff Fourier (e Å <sup>-3</sup> )	0.32
<i>R</i>	0.31
<i>R<sub>w</sub></i>	0.026
GOF	0.92
Full Data (4037 refls), MOLLY Refinement on <i>F</i> <sup>2</sup>	
highest peak diff Fourier (e Å <sup>-3</sup> )	0.22
<i>R</i>	0.0395
<i>R<sub>w</sub></i>	0.0386
GOF	2.67

of 3–50°, with a sealed Mo tube rated at 1.5 kW. The first set was collected at 216(1) K and the second at 180(1) K. Attempts to collect data at a temperature of 150 K were abandoned when it appeared that the crystal was slowly disintegrating. In each of the two cases, over a period of several months, 26 000+ reflections were measured to give ~5500 unique reflections with ~2500 observed [ $I > 3\sigma(I)$ ]. Preliminary results from these two data sets have been reported elsewhere.<sup>13,14</sup>

The third set of data was collected at 200(1) K on a RAXIS II-c diffractometer, with an area detector using a rotating-anode-generator X-ray source, over a range of  $\theta$  of 3–63° during a period of 6 h;<sup>14</sup> 17 639 reflections were recorded of which 4596 were unique (the completely unobserved reflections are not recorded) with 4038 observed [ $I > 3\sigma(I)$ ]. Full details are given in Table 1. The data were sorted to bring all the equivalent reflections together, and it was found for some weak reflections, where the same reflection had been observed more than three times, that one observation was significantly lower<sup>15</sup> (>10 esd's) than the others. In these instances, the anomalously weak reflection was removed from the data set and the merging *R* for all the data was then 0.027.

(ii) **Theoretical Calculations.** Theoretical electron density for just the phosphazene and aziridinyl rings were determined from *ab initio* calculations using GAMESS<sup>16</sup> with a 6-31G\* basis set. The deformation densities ( $\Delta\rho_m$ ) were derived from this according to the expression:<sup>17</sup>

$$\Delta\rho_m = \rho_{\text{molecule}} - \rho_{\text{SFA}}$$

where  $\rho_{\text{SFA}}$  is the density of the spherically averaged free atoms

(13) Cameron, T. S.; Borecka, B. *Phosphorus, Sulphur Silicon Relat. Elem.* 1992, 65, 121.

(14) Borecka, B.; Bakshi, P. K.; Cameron, T. S. *A.C.A. Conference Proceedings*; 1992; p 129. *Rigaku Journal* 1993, 10(2), 22.

superimposed on the molecular geometry. In this procedure, the electron density is calculated for the whole molecule with a 6-31G\* basis set and then the electron density is calculated for each atom in the exact position in the molecule again with a 6-31G\* basis set. Great care is taken here to ensure that the resulting density is spherically symmetric. The atomic densities are then subtracted from the molecular densities. Details of these calculations have been deposited.

### Structure Refinement

**Conventional Refinement.** While all three data sets give essentially the same results, this third set is clearly the most consistent, and it was used exclusively for the work reported here.<sup>18</sup>

The starting parameters were derived from previous low-temperature results, and after an initial refinement using all the observed data (details are given in Table 1), the parameters were then refined with just the reflections in the high-order (HO) range ( $\theta > 25^\circ$ ). The hydrogen atoms were placed in positions derived from neutron structures of similar molecules. One of the criteria used to establish which data set to use was the X–X<sub>HO</sub> maps calculated through the plane of the phosphazene and benzene rings. Those from data set 3 were clearly the best resolved and are shown in Figure 2.

**Multipole Refinement.** The aspherical atomic density  $\rho_r$  can be described in terms of spherical harmonics.<sup>19,20</sup>

$$\rho_{\text{atom}}(r) = \rho_{\text{core}}(r) + \rho_{\text{valence}}(r) + \rho_{\text{def}}(r)$$

Thus, for each atom

$$\rho_r = P_0\rho_c(r) + P_v(\kappa')^3\rho_v(\kappa'r) + \sum_{\ell} (\kappa'')^3 R_{\ell}(\kappa''r) \sum_{m=0}^{\ell} P_{\ell m} y_{\ell m}(\theta, \phi)$$

where the deformation term is in polar coordinates with the origin at the atomic nucleus.

The procedure for the use of this expression in refinement is now well established.<sup>21</sup> In this particular instance, the positional parameters and the anisotropic temperature factors of the heavy atoms were refined first using the high-angle data. The hydrogen atoms were adjusted to positions determined from neutron refinement of similar structures.<sup>22</sup> Then, the multipole parameters were refined with the atomic positions and the temperature factors fixed. The refinement showed a tendency to become unstable when the population and structural parameters were refined together. The phosphorus atom required hexadecapolar parameters ( $\ell = 4$ ), the remaining heavy atoms had octapolar parameters ( $\ell = 3$ ), and the hydrogen atoms had a simple dipole. In the multipole refinement, the results clearly showed mirror symmetry perpendicular to the plane of the aziridinyl group. A mirror plane of symmetry was imposed, by constraints, on each of the two aziridinyl groups. This mirror plane, perpendicular to the plane of the ring, contained the nitrogen atom and bisected the

(15) This observation has been commented on before, and there is not yet a generally accepted explanation. See, for example: Chidester, C. G.; Hann, F. S.; Watt, W. *A.C.A. Conference Proceedings*; 1993; p 38. However, in order to measure the reflections, a "frame" is placed round each observation to measure the reflection intensity within the frame and the background at the frame edge. With very weak reflections, the positioning of this frame may occasionally be incorrectly adjusted, either because the edge of the reflection is indistinct or because the reflection position has moved slightly from its expected position as the result of some minor mechanical/temperature control imperfection. Sato, M. *Rigaku Journal*, 1993, 10, 20. Rossman, M. G. *J. Appl. Crystallogr.* 1979, 12, 225.

(16) Schmidt, N. W.; Baldrige, K. K.; Boatz, J. A.; Jensen, J. H.; Koseki, S.; Gordon, M. S.; Nguyen, K. A.; Windus, T. L.; Elbert, S. T. *QCPE Bulletin* 1990, 10, 52.

(17) Smith, V. H.; Asbar, I. *Isr. J. Chem.* 1977, 16, 97, 87–102.

(18) A table of the results from the best of the sealed-tube data sets has been deposited.

(19) Stewart, R. F. *J. Chem. Phys.* 1969, 51, 4569.

(20) Hansen, N. K.; Coppens, P. *Acta Crystallogr.* 1978, A34, 909.

(21) See: *A.C.A. Transactions*; Blessing, R., Ed.; ACA: Buffalo, 1990; Vol. 26, seriatim.

(22) Allen, F. H.; Kennard, O.; Watson, D. G.; Brammer, L.; Orpen, A. G.; Taylor, R. *J. Chem. Soc. Perkin Trans. II* 1987, S1. Steiner, T.; Saenger, W. *Acta Crystallogr.* 1993, A49, 379.

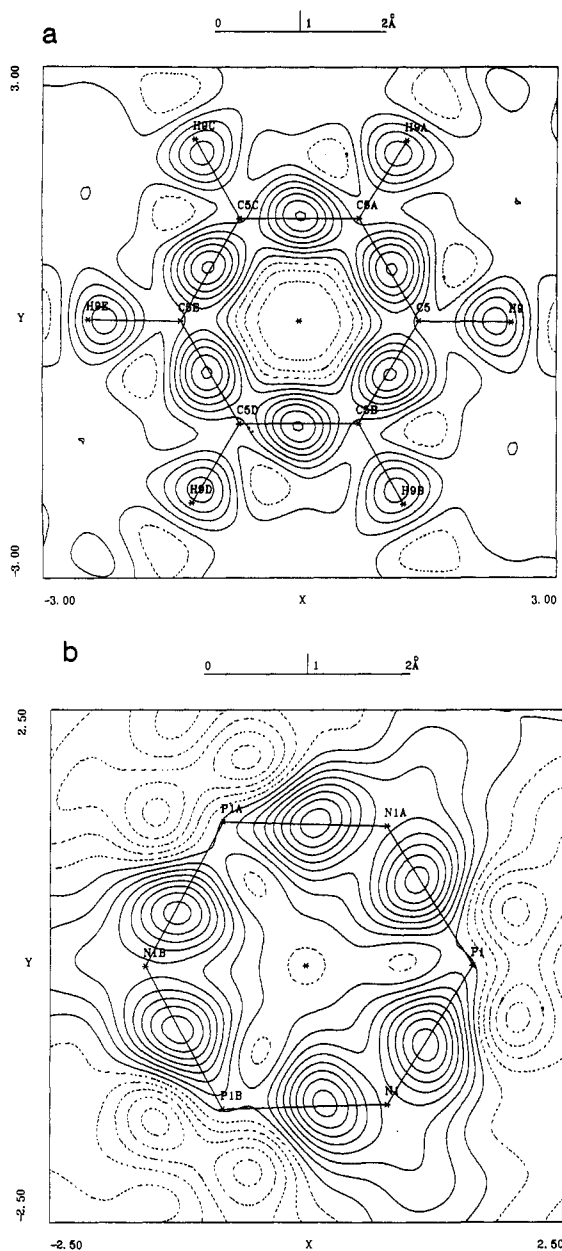


**Figure 2.** X-XHO electron density for (a) the plane of the benzene ring and (b) the plane of the phosphazene ring. Contours are at  $0.05 e/\text{\AA}^3$ . Zero and negative contour lines are broken.

C-C bond. Thus, the multipole parameters of C(1) were made equivalent, by  $C_s$  symmetry, to those of C(2), and similarly, the multipole parameters of C(3) were equivalent to those of C(4). Proper constraints were applied to the multipole parameters of N(1) and N(2) to maintain the  $C_s$  symmetry at these sites, too. When this refinement had converged, the multipole parameters were fixed and the positions and temperature factors (isotropic for hydrogen) of all atoms were refined for the full data. Finally, since the carbon atom of the benzene ring was only  $0.0033(10)$  Å from the best plane through the ring ( $D_{6h}$  symmetry within  $3.3\sigma$ ), the hydrogen atom of this ring was readjusted to a position determined from the neutron refinement. Similarly, the positions of the hydrogen atoms in the aziridinyl rings were also adjusted to positions of similar structures.<sup>22</sup> This adjustment was to accommodate any small alteration in the carbon positions in the final refinement. Details of the refinement are given in Table 1; the interatomic distances and the interbond angles are given in Table 2. The final calculated structure amplitudes  $F_c(\text{mult})$  were then used to calculate the *dynamic deformation* density maps

**Table 2.** Bond Lengths (Å) and Bond Angles (deg) (with esd's in parentheses from MOLLY refinement)

		Distances	
P(1)	N(1)	N(1)	1.587(1)
N(1)	P(1A)	P(1A)	1.601(1)
P(1)	N(1A)	N(1A)	1.601(1)
P(1)	N(2)	N(2)	1.675(1)
P(1)	N(3)	N(3)	1.680(1)
N(2)	C(4)	C(4)	1.464(1)
N(2)	C(3)	C(3)	1.478(1)
N(3)	C(2)	C(2)	1.472(1)
N(3)	C(1)	C(1)	1.476(1)
C(2)	C(1)	C(1)	1.474(2)
C(4)	C(3)	C(3)	1.484(1)
C(5)	C(5A)	C(5A)	1.391(2)
Angles			
N(1A)	P(1)	N(1)	117.00(5)
P(1A)	N(1)	P(1)	122.93(4)
N(1)	P(1)	N(2)	107.55(4)
N(1)	P(1)	N(3)	108.68(4)
N(2)	P(1)	N(3)	99.40(4)
P(1)	N(2)	C(4)	118.2(1)
P(1)	N(2)	C(3)	118.9(1)
C(4)	N(2)	C(3)	60.6(1)
P(1)	N(3)	C(2)	118.3(1)
P(1)	N(3)	C(1)	118.4(1)
C(2)	N(3)	C(1)	60.0(1)
N(3)	C(2)	C(1)	60.1(1)
N(3)	C(1)	C(2)	59.9(1)
N(2)	C(4)	C(3)	60.2(1)
N(2)	C(3)	C(4)	59.2(1)

using Fourier coefficients derived by:

$$F(\text{dynamic}) = F_c(\text{mult}) - F_c(\text{sph})$$

where  $F_c(\text{sph})$  is the structure factor calculated for spherical atoms for each atom,  $\kappa' = 1$ ,  $P_r$  is the number of valence electrons, and  $P_{e_m} = 0$ . The final multipole parameters are given in Table 3.

## Results and Discussion

(i) **The Benzene Ring.** The dynamic deformation density  $F(\text{dynamic})$  for the benzene ring is shown in Figure 3. Figure 3a shows the density in the plane of the ring, and Figure 3b shows the density in a plane perpendicular to the ring which bisects two opposite bonds and thus examines the  $\pi$  density above and below the ring plane. Figure 3c is the residual map which is almost featureless (see below). In these deformation density maps of benzene, the in-plane density closely resembles that observed in naphthalene.<sup>23</sup> The density, in a plane perpendicular to the ring plane, across the center of a bond has the elongation of the density in the direction of the  $\pi$  system. It is contracted, presumably by across-ring electron-electron repulsion, within the ring but extends more on the outside of the ring. This is exactly the expected picture. The residual map has one small feature at  $0.1 e/\text{\AA}^3$  on the C-C bond. The benzene molecule sits simultaneously with its center on both the 3-fold axis and the symmetry center, and thus, the whole ring is constructed from a single unique carbon-atom position. For the purposes of overdetermination of the structure, this is ideal, but any small deviation from perfect positioning of the ring, or deviation from  $D_{6h}$  symmetry of the carbon ring, is magnified by the center and then repeated by the 3-fold axis. Thus, this one small feature is not surprising.

(ii) **The Two Aziridinyl Groups.** The deformation densities for the two rings are shown in Figure 4: (a) in plane, (b) perpendicular to the ring plane which passes through the nitrogen atom and bisects the C-C bond, (c) the residual maps, and (d) the theoretically determined deformation map for the molecule HN-(CH<sub>2</sub>)<sub>2</sub>. The in-plane density maps are very similar for both unique rings and broadly resemble those observed<sup>11</sup> by Seiler *et*

(23) Brock, C. P.; Dunitz, J. D.; Hirshfeld, F. L. *Acta Crystallogr.* **1991**, *B47*, 789.

Table 3. Kappa, Scale Factor, Extinction, and Multipole Parameters

scale	extinction												
0.6037(3)	0.000												
$\kappa'$	$\kappa''$												
0.982(9)	0.717(15)	P(1)											
0.975(5)	0.731(28)	N(2)	N(3)										
1.002(5)	0.714(17)	C(2)	C(1)	C(4)	C(3)								
1.000	1.000	H(5)	H(7)	H(8)	H(3)	H(6)	H(1)	H(2)	H(4)	H(9)			
0.966(7)	0.541(22)	N(1)											
0.997(7)	0.746(25)	C(5)											

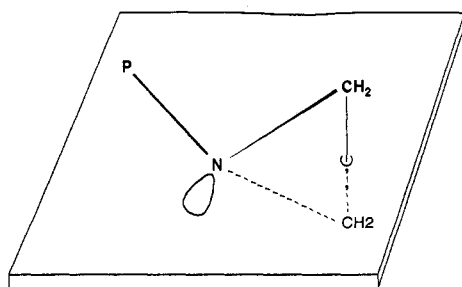
  

Multipole Parameters from MONOPOLE to 8-POL XX-YY													
atom	monopole	dipol X	dipol Y	dipol Z	4- POL ZZ	4- POL ZX	4- POL ZY	4- POL YY	4- POL XY	8- POL ZZZ	8- POL XZZ	8- POL YZZ	8- POL XX-YY
P(1)	4.50(19)	-0.08(7)	-0.12(13)	0.43(19)	0.21(8)	-0.05(5)	0.17(6)	0.09(5)	0.05(4)	0.84(6)	-0.05(4)	0.08(4)	-0.14(4)
N(1)	5.57(12)	-0.08(6)	0.33(11)	-0.37(18)	0.06(6)	0.01(5)	-0.20(5)	-0.13(4)	-0.20(3)	0.12(5)	-0.27(4)	0.09(5)	0.37(5)
N(2)	5.36(9)	-0.01(3)	-0.02(2)	0.00	-0.06(2)	0.00	0.00	0.05(2)	-0.07(2)	0.00	-0.14(2)	0.16(2)	0.00
N(3)	5.32(8)	-0.05(3)	-0.14(3)	0.00	-0.06(2)	0.00	0.00	0.09(2)	0.02(2)	0.00	-0.16(2)	0.17(2)	0.00
C(2) from C(1)													
C(1)	3.90(7)	-0.04(1)	-0.05(1)	0.10(2)	0.15(2)	0.03(2)	0.05(1)	0.08(1)	-0.06(1)	0.14(1)	0.12(2)	-0.05(1)	-0.22(1)
C(5)	4.01(6)	0.13(4)	-0.04(7)	-0.09(3)	0.04(2)	-0.09(2)	0.07(6)	-0.26(1)	-0.03(1)	0.20(2)	-0.19(6)	-0.05(10)	0.23(2)
C(4)	3.89(6)	0.04(1)	-0.05(1)	0.04(1)	0.19(2)	-0.05(2)	0.07(1)	0.06(1)	0.00(1)	0.20(1)	-0.02(1)	-0.07(1)	-0.16(1)
C(3) from C(4)													
H(5) from H(1)													
H(7) from H(1)													
H(8) from H(1)													
H(3) from H(1)													
H(6) from H(1)													
H(1)	0.96(1)	0.00(1)	0.02(1)	0.07(1)									
H(2) from H(1)													
H(4) from H(1)													
H(9)	1.05(5)	-0.03(3)	-0.13(4)	0.04(2)									

Multipole Parameters from 8-POL XYZ to 16-POL X3Y												
atom	8- POL XYZ	8- POL XXX	8- POL YYY	16- POL Z4	16- POL XZ3	16- POL YZ3	16- POL X2Y2	16- POL XYZ2	16- POL X3Z	16- POL Y3Z	16- POL X4 + Y4	16- POL X3Y
P(1)	0.01(4)	-0.11(3)	0.44(4)	0.07(3)	-0.04(2)	-0.08(2)	-0.04(3)	-0.29(3)	-0.01(2)	-0.18(3)	-0.11(2)	-0.07(2)
N(1)	-0.05(4)	-0.14(3)	0.20(3)									
N(2)	0.00	0.09(2)	0.06(1)									
N(3)	0.00	0.12(2)	0.03(1)									
C(1)	0.00(2)	-0.07(1)	0.18(1)									
C(5)	0.02(1)	-0.18(4)	-0.02(4)									
C(4)	-0.08(2)	0.04(1)	0.18(1)									

al. in cyclopropanes. The maxima of the ring-bond density lie outside the ring—the classical bent bond—though in both cases the density in the C–N bond is displaced from the center of the bond toward the more electronegative nitrogen atom. There are two odd little outlying peaks at the carbon atoms and a larger one at the nitrogen atom. These extra peaks were also seen by Seiler who quotes theoretical work<sup>24</sup> by Wiberg, Bader, and Lau to explain them. These features are also present in our own theoretical deformation density maps (see below). The plane perpendicular to the ring plane which passes along the N–P bond and bisects the C–C bond should also contain the lone pair of electrons on the nitrogen atom(III). Thus, the bonding density



(III)

in the P–N bond should be clearly seen, and the lesser lone-pair density should occur about 0.6 Å from the nitrogen atom on the

(24) Wiberg, K. B.; Bader, R. F. W.; Lau, C. D. H. *J. Am. Chem. Soc.* 1987, 109, 985 and references therein.

angle bisector of the P–N bond and the line from nitrogen to the center of the C–C bond. Again, while the precise details vary between the two rings, this is exactly what is observed, with the distance of the lone-pair density maximum between 0.5 and 0.6 Å from the nitrogen atom. The residual map for one of the rings shows a feature at 0.2 e/Å<sup>3</sup> which is larger than one would like. However, as explained in the Experimental Section above, the two carbon atoms were refined in the multipole model as though they were chemically equivalent. Clearly, if the refinement is correct, they are indeed very nearly equivalent—too closely equivalent to be refined separately—but from Figure 1, it is clear that the two carbon atoms are, in fact, in distinguishable chemical environments. Carbon atoms C(1) and C(3) are toward the center of the molecule, close to an extension of the phosphazene ring plane, and C(2) and C(4) are to the outside of the molecule. Further, C(2), together with its hydrogen atoms, takes part in trapping the benzene molecule between itself (with a 3-fold generation) and the centrosymmetrically related group (Figure 1a), while C(4) meshes with its centrosymmetric (and 3-fold) related equivalents and holds two adjacent phosphazene molecules in place. Thus, the 0.2 e/Å<sup>3</sup> feature on the residual map can be explained by very small nonequivalence of the chemical environment of the two carbon atoms of the ring.

The theoretical deformation density was calculated for the simple cyclic amine HN(CH<sub>2</sub>)<sub>2</sub>, and this is shown in Figure 4d. While there are some small differences between the experimental and theoretical deformation maps, they are essentially similar. Any differences are within the variation expected between the aziridinyl group on the phosphazene ring and the simple unsubstituted cyclic amine of the theoretical calculation.

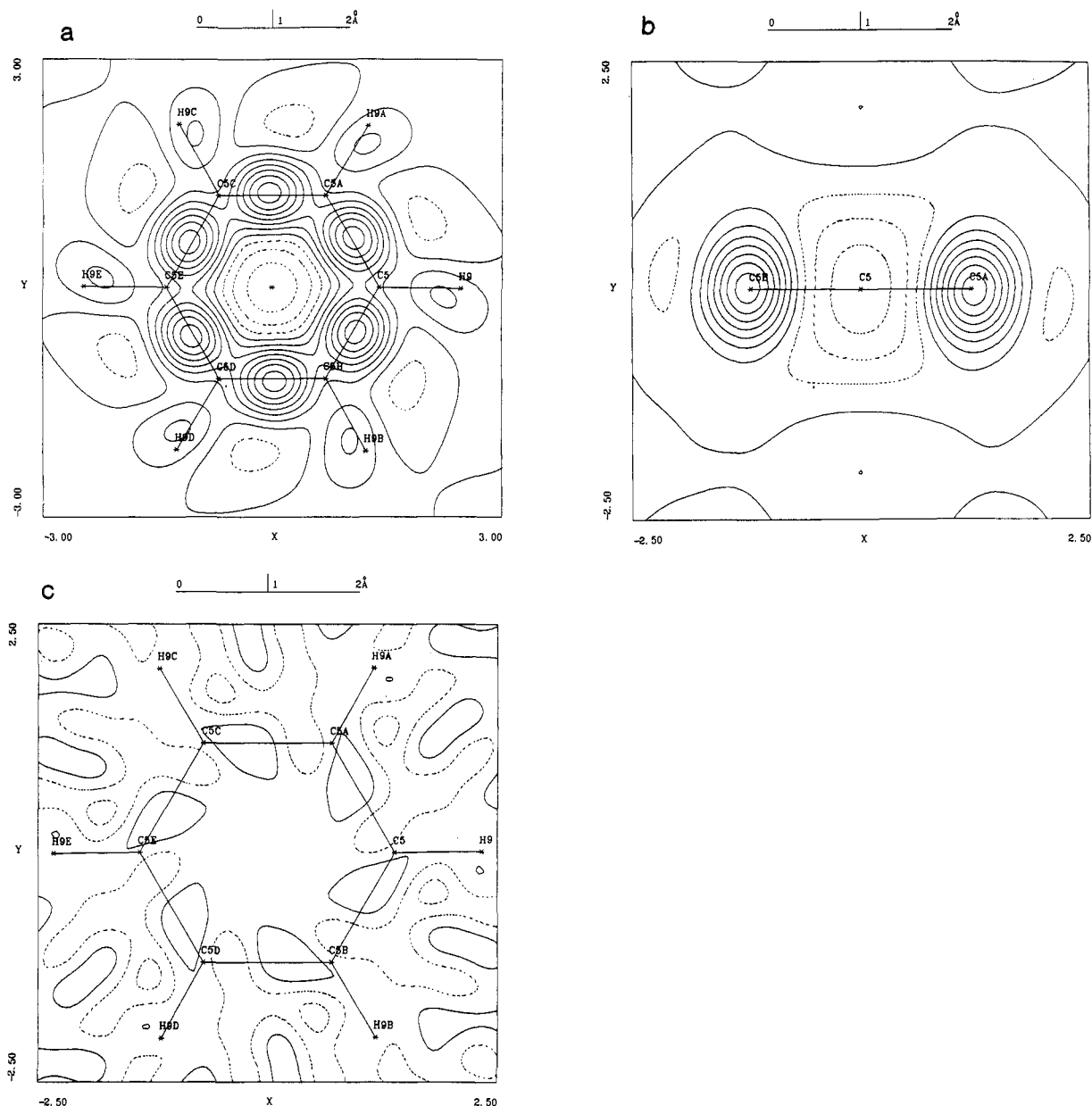
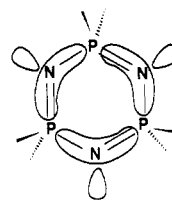


**Figure 3.** Dynamic deformation density maps for benzene (a) in the plane of the ring and (b) perpendicular to the plane of the ring bisecting two opposite bonds (contours for (a) and (b) at  $0.05 \text{ e}/\text{\AA}^3$ ) and (c) the residual map with contours at  $0.1 \text{ e}/\text{\AA}^3$ . Zero and negative contour lines are broken.

(iii) **The Phosphazene Ring.** An essential prerequisite for the consideration of the bonding density in the phosphazene ring was that the densities observed for the benzene and aziridinyl rings should be well defined, consistent, and as expected. This has now been established. The corresponding densities for the phosphazene ring are shown in Figure 5. It can be seen from the ring-plane densities (Figure 5a) that there is a node at each phosphorus atom and that the electron density spreads from one P–N bond through the nitrogen to the second N–P bond. This is exactly as predicted by Dewar's island delocalization model. Further, there is a considerable spread of electron density inside and in the plane of the ring as is expected for the  $\pi'$  bonding. This can be seen both in the ring-plane diagram (a) and in the plane perpendicular to this which bisects two opposite P–N and N–P bonds (b). The effect would be much more marked in (b) if the chosen plane ran through the maxima of the bonding density of the opposite P–N and N–P bonds. Figure 5c shows a plane perpendicular to the ring plane which bisects the P–N–P angle, and here, the nitrogen lone-pair electron density can be seen between  $0.5$  and  $0.6 \text{ \AA}$  from the nitrogen atom (IV).

The residual map (Figure 5d) shows some features which just rise to  $0.2 \text{ e}/\text{\AA}^3$ . The ring here is generated from one unique phosphorus atom and one unique nitrogen atom by the 3-fold



(IV)

axis, and as with benzene, any small real deviation from this has not been taken into account. If any significance is placed on these residuals it would seem that our model has been unable to match exactly the geometric requirements of the contribution from the  $\pi'$  bonding. Theoretical deformation densities were calculated for the cyclic phosphazene  $(\text{H}_2\text{PN})_3$ , and the density in the ring plane is shown in Figure 5e. As with the aziridinyl groups, the experimental and theoretical density maps are essentially the same.

#### Summary

The deformation densities of a benzene ring, two aziridinyl rings, and a phosphazene ring, which have not been observed

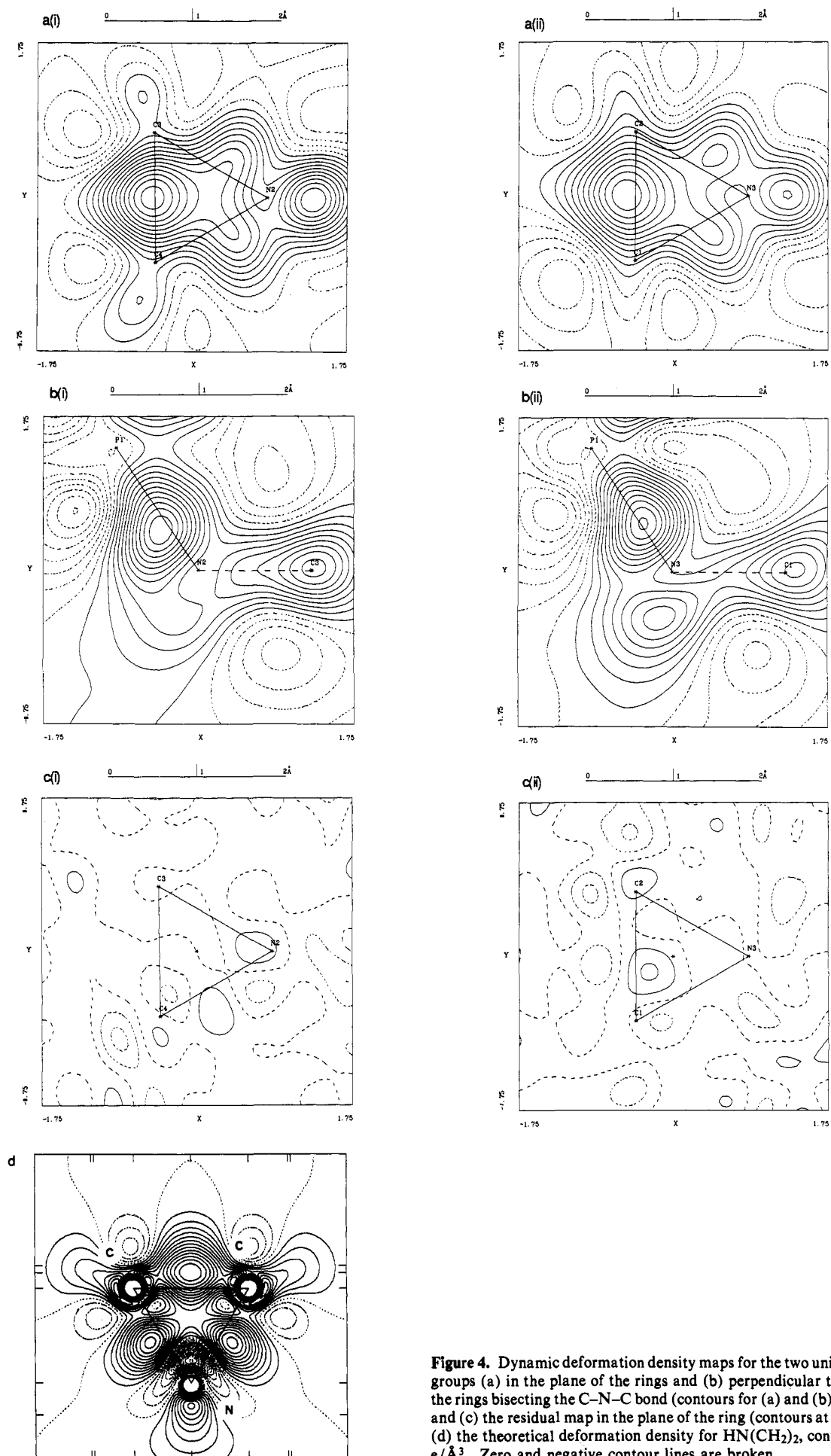


**Figure 4.** Dynamic deformation density maps for the two unique aziridiny groups (a) in the plane of the rings and (b) perpendicular to the plane of the rings bisecting the C–N–C bond (contours for (a) and (b) at  $0.02 \text{ e}/\text{\AA}^3$ ) and (c) the residual map in the plane of the ring (contours at  $0.1 \text{ e}/\text{\AA}^3$ ) and (d) the theoretical deformation density for  $\text{HN}(\text{CH}_2)_2$ , contours at  $0.005 \text{ e}/\text{\AA}^3$ . Zero and negative contour lines are broken.

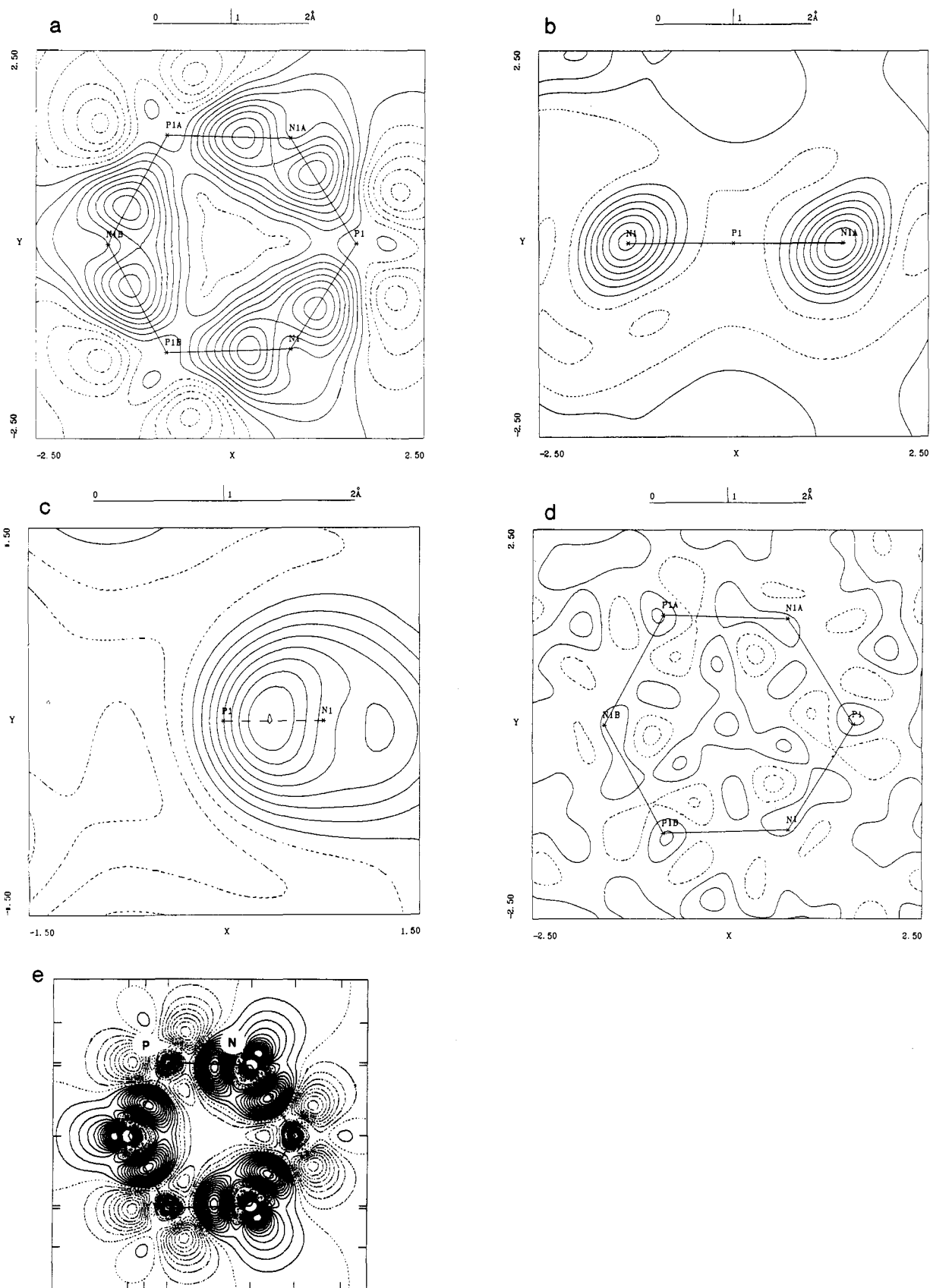


**Figure 5.** Dynamic deformation density maps for the phosphazene ring (a) in the plane of the ring, (b) perpendicular to the plane of the ring bisecting two opposite P–N and N–P bonds (contours for (a) and (b) at  $0.05 \text{ e}/\text{\AA}^3$ ), and (c) perpendicular to the plane of the ring bisecting a ring P–N–P bond (contours at  $0.03 \text{ e}/\text{\AA}^3$ ) and (d) the residual map with contours at  $0.1 \text{ e}/\text{\AA}^3$  and (e) the theoretical deformation density for  $(\text{H}_2\text{PN})_3$ , contours at  $0.005 \text{ e}/\text{\AA}^3$ . Zero and negative contour lines are broken.

before, have been examined all in one crystal. The observed densities of the benzene and aziridinyl rings are consistent and as expected. The deformation density of the cyclotriphosphazene

ring has been examined in the context of the observations on the other rings and found to be as predicted by earlier theoretical work. The experimental deformation densities on the phosphazene



and aziridinyl rings have been compared with those calculated theoretically for the simple rings alone and found to be essentially the same.

Work is now starting on the deformation density studies of  $P_3N_3AZ_5Cl$  and on *gem*- $P_3N_3Cl_4AZ_2$  to see whether the well-documented,<sup>6</sup> substituent-induced variation in ring P-N bond lengths is also reflected in the bond deformation densities. Work is also in progress<sup>25</sup> on the deformation density of a compound containing the three-membered diazine ( $>CN_2$ ) ring for comparison with the aziridinyl system.

**Acknowledgment.** The authors are grateful to Molecular Structure Corporation who provided the essential support by

(25) Cameron, T. S.; Bakshi, P. K.; Borecka, B.; Liu, T. H. M. *J. Am. Chem. Soc.* **1992**, *114*, 1889.

collecting the data for this work. They also acknowledge the support of the Killam Foundation for a scholarship (B.B.).

**Supplementary Material Available:** Tables of fractional coordinates and thermal parameters, summaries of *ab initio* calculations, a diagram showing the thermal ellipsoids, and a summary table for the analysis of the sealed-tube data collection at 180 K (11 pages); structure factors (9 pages). This material is contained in many libraries on microfiche, immediately follows this article in the microfilm version of the journal, and can be ordered from the ACS; see any current masthead page for ordering information.